MOLECULAR AND CELLULAR BIOLOGY, Jan. 1995, p. 315–325 Vol. 15, No. 1
0270-7306/95/$04.00+0
Copyright © 1995, American Society for Microbiology

A New Platelet-Derived Growth Factor-Regulated Genomic Element Which Binds a Serine/Threonine Phosphoprotein Mediates Induction of the Slow Immediate-Early Gene *MCP-1*

ROLF R. FRETER, JOHN A. ALBERTA, KAI KAI LAM, AND CHARLES D. STILES*

Department of Microbiology and Molecular Genetics, Division of Clinical Oncology, and Division of Cellular and Molecular Biology, Harvard Medical School and Dana-Farber Cancer Institute, Boston, Massachusetts

Received 30 March 1994/Returned for modification 16 May 1994/Accepted 18 October 1994

The *MCP-1* chemokine gene belongs to a cohort of immediate-early genes that are induced with slower kinetics than c-*fos*. In this study, we identified a cluster of four platelet-derived growth factor (PDGF)-responsive elements within a 240-bp enhancer found in the distal 5′ flanking *MCP-1* sequences. Two of the elements bind one or more forms of the transcription factor NF-κB. We focused on the other two elements which are hitherto unreported, PDGF-regulated genomic motifs. One of these novel elements, detected as a 28-mer by DNase I footprinting, restores PDGF inducibility when added in two copies to a 5′ truncated *MCP-1* gene. A single copy of the second novel element, a 27-mer, restores PDGF inducibility to a 5′ truncated MCP-1 gene. The 27-base element interacts with a PDGF-activated serine/threonine phosphoprotein that is detected only within the nucleus of PDGF-treated 3T3 cells. DNA binding of this phosphoprotein is activated by PDGF treatment with slow kinetics that match the time course of *MCP-1* gene expression, and activation is not inhibited by cycloheximide. PDGF-activated binding to the 27-mer is shown to involve a single 30-kDa protein by UV-cross-linking analysis.

Serum growth factors stimulate expression of the immediate-early gene set within their target cells. By definition, immediate-early genes are induced at the transcriptional level by growth factors, and the induction is not blocked by drugs that inhibit protein synthesis (1, 23, 27, 28, 41). Because all components of the transcriptional response preexist within cells, *cis*- and *trans*-acting regulatory elements for the immediate-early genes define useful endpoints for analysis of signal transduction. A well-characterized example of a fast immediate-early gene is c-*fos*. A cluster of three *cis*-acting regulatory elements contained within the proximal 5′ flanking sequences of c-*fos* has proven to be of general interest for problems in growth factor signal transduction. The three functionally distinct elements within the proximal 5′ flanking sequences of c-*fos* include a 22-nucleotide region of dyad symmetry, termed the serum response element, a cyclic AMP response element, and an element responsive to platelet-derived growth factor (PDGF) B:B homodimers known as the sis-inducible element (4, 12, 14–16, 44, 47, 48, 50, 51). Nuclear *trans*-acting proteins that interact with these *cis*-acting regulatory elements have been isolated and characterized (10, 31, 32, 35, 36, 49). By both sequence analysis and functional analysis, the regulatory elements defined initially within c-*fos* have been detected within other immediate-early genes (7, 33, 37).

The c-*fos* gene, however, does not stand as a prototype for all members of the immediate-early gene set. A second cohort of the immediate-early gene set is induced with slower kinetics than c-*fos* and by distinctly different mechanisms (20, 21). The first proto-oncogene (c-*myc*) (25) and the first chemokine gene (*JE*/*MCP-1*, hereafter referred to as *MCP-1*) (8, 39, 40) described are contained within this subset, which we refer to as slow immediate-early genes. PDGF added to quiescent 3T3 cells stimulates transcription of c-*fos* within 10 min. c-*fos* transcripts reach peak levels within 30 min and return to baseline within 2 h (17, 26). In contrast to the rapid but transient response exhibited by c-*fos*, slow immediate-early genes like c-*myc* and *MCP-1* display a 60- to 90-min lag time for initiation of transcription (9, 18, 26). Nuclear runoff transcription analysis demonstrates that induction of *MCP-1* mRNA by PDGF and serum is primarily the result of increased transcription (18, 20, 24, 38). No *fos*-like regulatory elements are found within several kilobases of 5′ or 3′ flanking sequences of the *MCP-1* gene or within its coding sequences. A major bottleneck for structure-function analysis of the slow immediate-early genes has been obtaining regulated expression in transient transfection studies.

We recently reported a discontiguous pair of *cis*-acting elements, both of which are essential for regulated expression of the murine *MCP-1* gene. One of these elements is a 7-base motif, TTTTGTA, located in the proximal 3′ *MCP-1* untranslated sequences. The mechanism of action of this 3′ element is unknown. However, identical 7-mers are found in proximal 3′ untranslated sequences of c-*myc*, multiple zinc finger transcription factor genes, and multiple cytokines belonging to the immediate-early gene set (13). The discovery of the essential 3′ 7-mer facilitated detection of a second required *MCP-1* genomic element. The second element was detected as a 240-bp fragment found 2.3 kb upstream of the *MCP-1* start of transcription. The 240-bp fragment is sufficient to restore PDGF inducibility (provided that the 3′ 7-mer is also present) in a position- and orientation-independent manner; i.e., it functions as a classical inducible enhancer element (13). Furthermore, the 240-bp fragment is sufficient to restore induction of the *MCP-1* gene in response to serum, double-stranded RNA, interleukin-1α (IL-1α) or PDGF (13).

In this report we show that four distinct PDGF-regulated elements are present within the 240-bp enhancer fragment. Two of the elements contain homologous sequences and bind several forms of the transcription factor NF-κB. Herein we

* Corresponding author. Mailing address: Dana-Farber Cancer Institute, 44 Binney St., Boston, MA 02115. Phone: (617) 632-3511. Fax: (617) 632-4663.

TABLE 1. Double-stranded oligonucleotides used in this study[a]

Element	Sequence
I	5′-GGGCCTTTCCCTTGGCTGCTCCCAAG
II	5′-CCTTTGTTGAGTCATTTCAGATTCTCC
II (mut1)	5′-ATCGGTCGGAGTCATTTCAGATTCTCC
II (mut2)	5′-CCTTTGTTGAGTACCGCACTATTCTCC
III	5′-AGAACTGCTTGGCTGCAGGCCCAGCATC
III mut	5′-AGAACTGCTTGTAGTACTTCCCAGCATC
IV	5′-AGAATGGGAATTTCCACGCTCT
NF1	5′-GGGACTTTCCGGGACTTTCC
NF2	5′-GGGAACTTCCGGGAACTTCC
4×7	5′-TTTTGTATTTTGTATTTTGTATTTTGTA

[a] All sequences shown are of the top strand. Mutations of element II and III sequences are underlined.

focus on the other two elements, which appear to be previously uncharacterized, PDGF-regulated protein-binding sequences.

MATERIALS AND METHODS

Growth factors and reagents. The recombinant B:B isoform of PDGF and recombinant IL-1α were obtained from Upstate Biotechnology, Inc. RNase A was obtained from Pharmacia. Proteinase K, RNase T_1, calf intestinal phosphatase (CIP), and poly(dI-dC) were obtained from Boehringer Mannheim Biochemicals. Bovine calf serum was obtained from Hyclone. Human defibrogenated platelet-poor plasma (PPP) was prepared as described previously (34). Monoclonal antibodies to phosphoserine, phosphothreonine, and phosphotyrosine were obtained from Sigma. Polyclonal antibodies to the p50 and p65 subunits of NF-κB, and the peptides that these antibodies were raised against, were obtained from Santa Cruz Biotechnology. Synthetic oligonucleotides were obtained from Macromolecular Resources. Tyrosine phosphatase from *Yersinia enterocolitica* was obtained from New England Biolabs.

Cell culture, DNA transfections, stimulation assays, and RNA preparation and analysis. NIH 3T3 cells were maintained in Dulbecco's modified Eagle medium (DME medium; Gibco Laboratories) supplemented with 10% bovine calf serum. NIH 3T3 cells were used for transient transfections because of their significantly greater transfection efficiency compared with BALB/c-3T3 cells. Twenty hours prior to transfection, cells were plated at a density of 2.0×10^6 per 15-cm-diameter tissue culture dish. Calcium phosphate-mediated DNA transfections were performed as described previously (14), with the following modifications. Cells were exposed to DNA-containing precipitates for 6 h followed by a 2-min 20% glycerin shock. Cells were then washed with DME and placed in DME plus 5% PPP. Because of variable background levels of *MCP-1* transcripts in transfected cells quiesced with 0.5% calf serum, we have found it more useful to use 5% PPP in quiescing transfected cells after the glycerin shock. Transfection mixtures included 50 μg of tagged *MCP-1* reporter constructs together with 10 μg of an alpha-globin reference construct (pSVα-1), a gift from M. Greenberg (Harvard Medical School), per 15-cm-diameter tissue culture plate. After 40 to 44 h in 5% PPP, stimulated groups of cells were exposed to the B:B isoform of PDGF (30 ng/ml) for 2 h, unless otherwise indicated in the figure legends. Total RNA was prepared by the guanidinium isothiocyanate method and purified on CsCl gradients (5).

Total RNA samples (30 μg per assay for transient transfections and 10 μg per assay for endogenous *MCP-1* analysis) were analyzed by RNase protection assay as described previously (52). RNase treatment was done with 60 μg of RNase A per ml and 2 μg of RNase T_1 per ml for 75 min at 35°C. Nuclease-resistant fragments were separated on 8-mm 6% polyacrylamide–8 M urea gels. Synthesis of labelled complementary RNA probes was done as described previously (30), with pGEM vectors (Promega). Probes were gel purified before use. The probe for tagged *MCP-1* expression is a 272-bp *Hin*cII *MCP-1* cDNA fragment spanning portions of the second and third exons. The fragment is elongated by the addition of a 33-bp tag into a blunted *Sau*I site and inserted into the *Sma*I site of pGEM 7 (13). The length of the unprotected probe is 377 bases. As a control for equal transfection efficiencies between groups of cells, 10 μg of total RNA was assayed by RNase protection for the presence of a constitutively active cotransfected alpha-globin construct. Exposure and quantitation of gels were done for all experiments on a PhosphorImager (Molecular Dynamics).

Oligonucleotides. The double-stranded oligonucleotides containing 5′ overhanging GG (top strand) and CC ends (bottom strand) used are shown in Table 1.

Preparation of nuclear and cytoplasmic extracts and electrophoretic mobility shift assays. Nuclear and cytoplasmic S100 extracts from BALB/c-3T3 fibroblasts (clone A31) were prepared as described by Dignam et al. (11). Chemically synthesized oligonucleotides were annealed and labelled with ^{32}P-nucleotides by fill-in with the Klenow fragment of DNA polymerase I. Radiolabelled double-stranded oligonucleotides were gel purified prior to use as probes in electrophoretic mobility shift assays. Binding reaction mixtures contained 10 to 15 μg of fibroblast nuclear extracts, radiolabelled oligonucleotide probe (10,000 cpm; 0.1 to 0.25 ng), and 0.5 or 1.5 μg of (element III only) poly(dI-dC) in 10 mM Tris (pH 7.5)–5% (vol/vol) glycerin–50 mM NaCl–1 mM EDTA–1 mM dithiothreitol in a final volume of 20 μl. Following 50 or 15 min (element III only) of incubation on ice, DNA-protein complexes were electrophoresed on 4% native polyacrylamide gels at 150 V for 2.5 h at room temperature in 0.25× TBE (Tris-borate-EDTA) buffer. For antibody supershift or competition experiments, antibodies or 100-fold excesses of unlabelled oligonucleotides were added for a 30-min incubation on ice prior to the addition of the radiolabelled oligonucleotide probe.

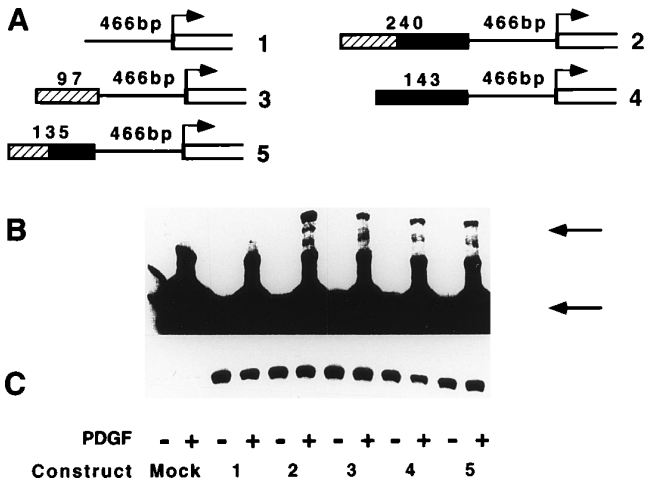

FIG. 1. PDGF induction of *MCP-1* involves at least two distinct elements within a 240-bp enhancer fragment. (A) Schematic diagram (construct 1) of the structure of the 5′ end of a noninducible tagged MCP-1 reporter gene (pGMJE-1), which includes 466 bp of the 5′ flanking sequences and 1.9 kb of the 3′ untranslated sequences. All additional constructs are derived from construct 1 by readdition of the shown 240-, 97-, 143-, and 135-bp fragments (constructs 2, 3, 4, and 5, respectively). The 240-bp fragment is present in the distal 5′ *MCP-1* flanking sequences (with ends at −2537 and −2298 bp relative to the *MCP-1* start of transcription). The 97- and 143-bp fragments are nonoverlapping subfragments of the 240-bp fragment. The 135-bp fragment (including nucleotides 34 through 168 of the 240-bp fragment) overlaps both the 97- and 143-bp fragments. All fragments were readded in the in vivo orientation. (B) RNase protection assays of 30 μg of total cellular RNA from fibroblasts either transfected with 50 μg of the shown constructs or mock transfected, allowed to become quiescent, and then either not exposed (−) or exposed (+) to the B:B isoform of PDGF (30 ng/ml) for 2 h. The arrows highlight the 305-nucleotide (top arrow) and 241-nucleotide (bottom arrow) protected fragments corresponding to expression of transfected *MCP-1* constructs and endogenous *MCP-1*, respectively. PhosphorImager images were designed to optimally demonstrate expression of the transfected constructs. Equal inductions of construct 2 and endogenous *MCP-1* were observed in all experiments. (C) RNase protection assays of 10 μg of total cellular RNA from the transfections shown in panel B with an alpha-globin riboprobe.

UV cross-linking and DNase I footprinting. UV cross-linking was performed as described previously (6). Native polyacrylamide gels used for cross-linking experiments were run at 150 V at 4°C in 0.25× TBE buffer. DNase I footprinting was performed as described previously (2), with the following modifications. A PDGF-regulated 240-bp *Sma*I-*Hin*cII *MCP-1* genomic fragment (13) inserted into the *Sma*I site of pGEM-7 was used to generate single-strand ^{32}P-labelled nucleotide probes by fill-in with the Klenow fragment of DNA polymerase I. Footprinting reaction mixtures included 150 μg of fibroblast nuclear extracts, 3.3 μg of poly(dI-dC), and single-strand radiolabelled probes (20,000 cpm), with the same binding buffer used for electrophoretic mobility shift assays in a final volume of 50 μl. After a 30-min incubation on ice, 3 U of DNase I (Promega) was added at room temperature for 1 min. The Mg^{2+} and Ca^{2+} concentrations of all footprinting reaction mixtures were adjusted to 5 and 2 mM, respectively, immediately after the addition of DNase I. Following phenol extraction and ethanol precipitation, DNase I digestion reaction mixtures were electrophoresed on 6% acrylamide–8 M urea sequencing gels.

Plasmid construction. A murine *MCP-1* genomic clone (pGMJE-1) with 466 bp of 5′ flanking sequences and 1.9 kb of 3′ flanking sequences was a gift from B. Rollins (Dana-Farber Cancer Institute). The *MCP-1* construct was originally inserted into the *Eco*RI site of pGEM-1 (39). A noninducible tagged *MCP-1* construct (construct 1 in Fig. 1 and 6) was created by blunt ligation of a 33-bp

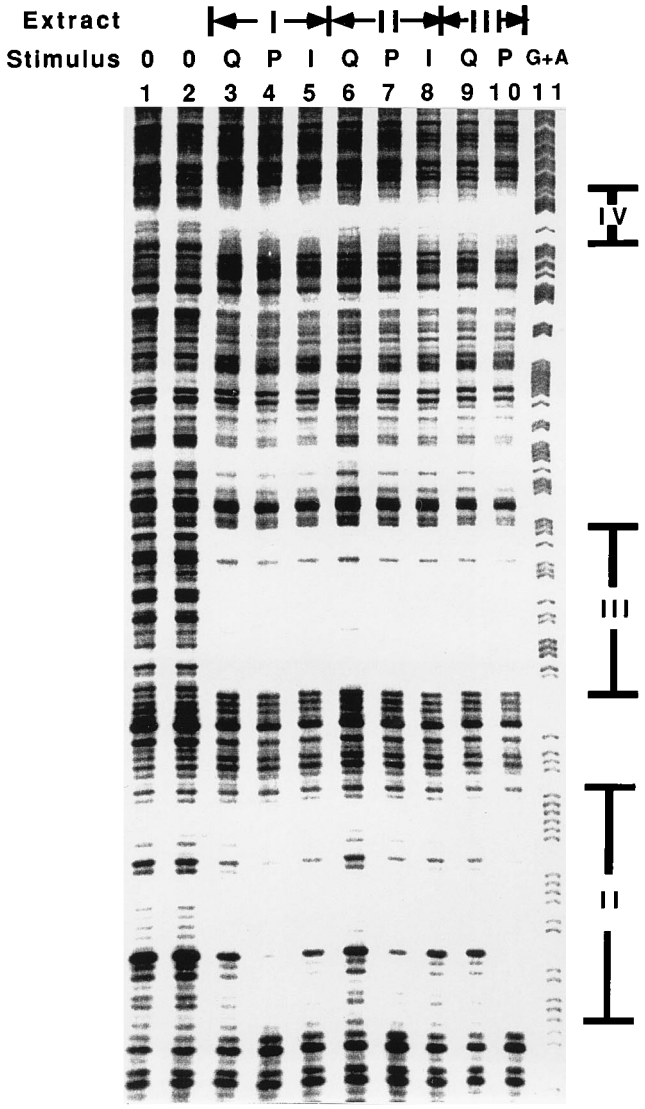

FIG. 2. Multiple PDGF-regulated *cis*-acting elements are detected by DNase I footprinting. A radiolabelled probe corresponding to the bottom strand of the 240-bp *MCP-1* enhancer was used in DNase I footprinting analysis with three nuclear extracts from quiescent fibroblasts (Q) or fibroblasts treated for 1.75 h with either 30 ng of the B:B isoform of PDGF (P) per ml or 10 ng of IL-1α (I) per ml. Nuclear extracts were prepared by the method of Dignam et al. (11) from three separate groups of BALB/c-3T3 cells otherwise grown and quiesced in identical fashion. Lanes: 0, no protein; G+A, purine sequence of the radiolabelled bottom-strand probe. Protected regions corresponding to elements II, III, and IV are indicated on the right. Corresponding footprints were detected by using a radiolabelled top strand of the 240-bp *MCP-1* enhancer (data not shown).

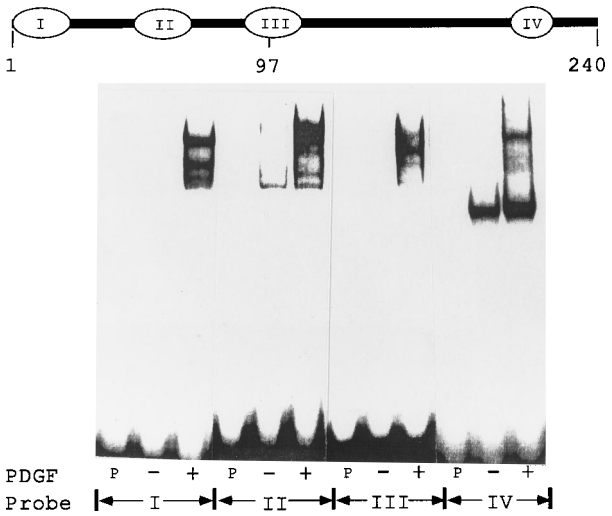

FIG. 3. PDGF inducible complexes are detected in mobility shift assays using oligonucleotide probes corresponding to each of the four *cis*-acting elements. Shown at the top in schematic form is the 240-bp *MCP-1* enhancer fragment. Position 1 is at the 5′ end of the fragment. The relative positions of the four elements with respect to the nonoverlapping 97- and 143-bp subfragments are shown. Radiolabelled double-stranded oligonucleotide probes, corresponding to the genomic elements detected in Fig. 2, were used individually in mobility shift assays with 15 μg (elements I, II, and IV) or 10 μg (element III) of nuclear extracts prepared from quiescent fibroblasts (−) or fibroblasts treated with the B:B isoform of PDGF (30 ng/ml) for 1.75 h (+). P denotes probe alone.

*Xho*I-*Cla*I fragment of the pGEM-7 polylinker to a *Sau*I site in the third exon of pGMJE-1 (1,049 nucleotides downstream of the transcription start site). An identical 33-bp tag was inserted into the RNase protection probe vector described above.

Add-back constructs shown in Fig. 1 and 6 were generated by blunt ligation of *MCP-1* genomic sequences or double-stranded synthetic oligonucleotides to tagged pGMJE-1 (construct 1 in Fig. 1 and 6) opened with *Sal*I. Construct 2 in Fig. 1 and 6 was generated by blunt ligation of a 240-bp *Sma*I-*Hin*cII *MCP-1* fragment (with ends at −2537 and −2298 bp relative to the *MCP-1* start of transcription) to *Sal*I-opened construct 1. Constructs 3, 4, and 5 in Fig. 1 were generated by blunt ligations of 97-bp *Sma*I-*Pst*I, 143-bp *Pst*I-*Hin*cII, and 135-bp *Dde*I subfragments of the 240-bp fragment to *Sal*I-opened construct 1, respectively. Constructs 3 through 9 in Fig. 6 (top) and the two mutants in Fig. 6 (middle) were generated by blunt ligations of the relevant double-stranded synthetic oligonucleotides corresponding to the wild-type and mutant elements II and III to *Sal*I-opened construct 1. All constructs were checked for accuracy by DNA sequencing (43).

RESULTS

PDGF induction of *MCP-1* involves at least two distinct elements within the distal 240-bp enhancer fragment. Initial experiments were designed to locate a PDGF-responsive genomic element(s) within the 240-bp enhancer fragment. Three subfragments of the 240-bp enhancer fragment were generated, including the distal 97 nucleotides, the proximal 143 nucleotides, and a 135-nucleotide subfragment which overlaps the distal and proximal subfragments (Fig. 1A, constructs 3, 4, and 5, respectively). Readdition of any subfragment restores PDGF inducibility to a truncated *MCP-1* reporter construct in transient transfection experiments (Fig. 1B). Significantly, however, only 30 to 50% of the induction observed with the full 240-bp enhancer is obtained with any one of the subfragments (Fig. 1B). Since constructs 3 and 4 are both PDGF inducible but contain nonoverlapping subfragments of the 240-bp enhancer, these data demonstrate that at least two PDGF-responsive elements are present within the 240-bp genomic enhancer.

DNase I footprinting and mobility shift assays highlight four PDGF-responsive elements within the 240-bp enhancer fragment. Three regions (designated elements IV, III, and II in Fig. 2 and all subsequent figures) are protected from DNase I digestion by nuclear extracts from PDGF-treated fibroblasts. An additional element (element I in all subsequent figures) is located at the extreme 5′ terminus of the 240-bp fragment and was detected by its close sequence homology to element IV. Footprints corresponding to elements II and IV display both constitutive and PDGF-inducible components (Fig. 2, compare lanes 4, 7, and 10 with lanes 3, 6, and 9, respectively). In BALB/c-3T3 cells, the *MCP-1* gene is also induced by IL-1α (13, 19). For comparative purposes, we conducted footprint

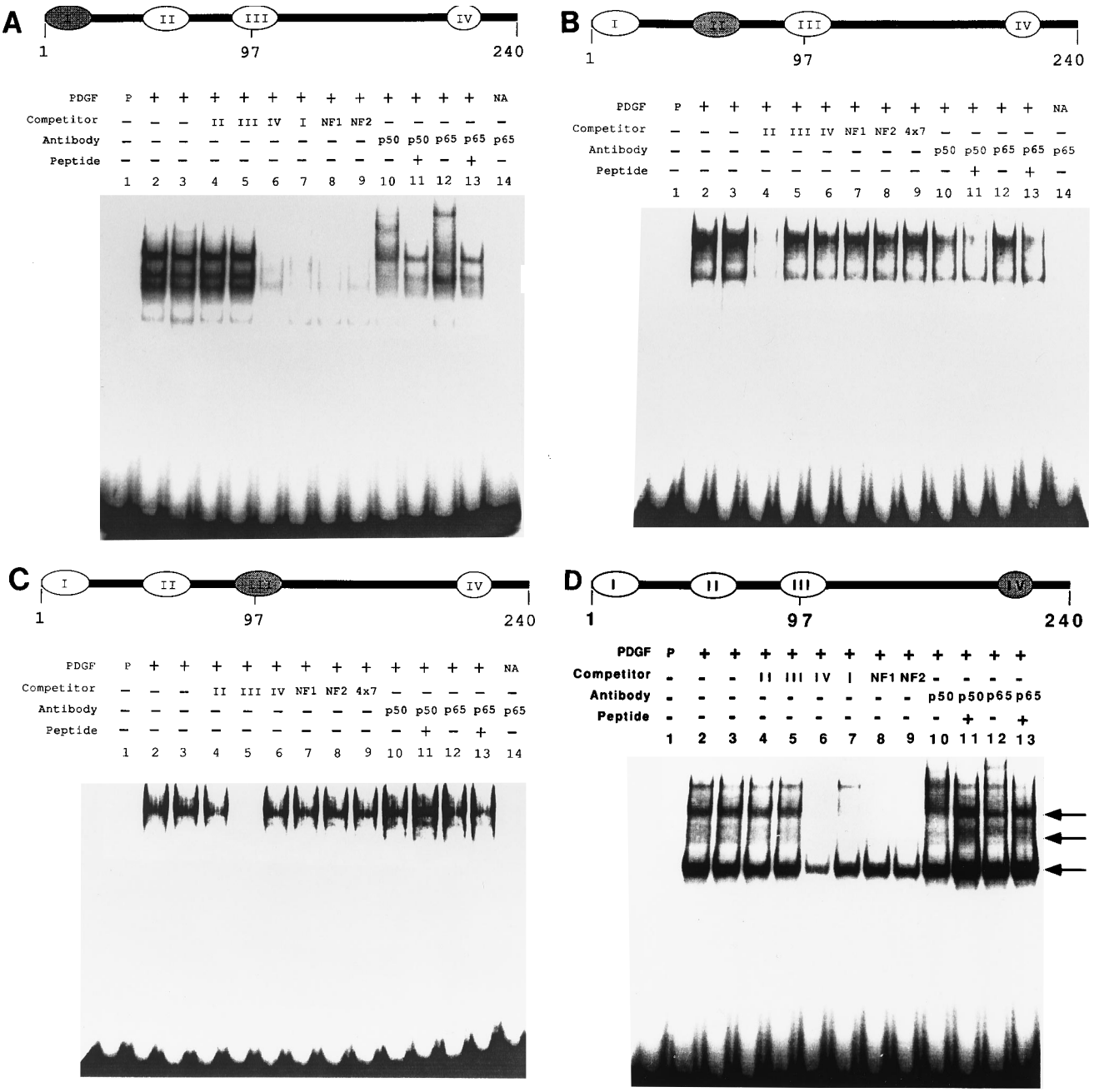

FIG. 4. Characterization of the four *MCP-1* genomic elements by competition analysis and antibody supershifts in mobility shift assays. A schematic diagram of the 240-bp *MCP-1* enhancer fragment is shown at the top of each panel. Position 1 is at the 5′ end of the fragment. The relative positions of the four elements with respect to the nonoverlapping 97- and 143-bp subfragments are shown. A shaded oval denotes the probe used in the mobility shift assays shown in each panel. Sequences of all double-stranded oligonucleotides used in competition assays are given in Materials and Methods. Double-stranded oligonucleotide competitors were added in 100-fold excess for all competition assays. Rabbit polyclonal antibodies (2.5 μg) raised against the 50-kDa subunit (p50) or 65-kDa subunit (p65) of NF-κB were used for supershifts. Control peptides for each antibody (1 μg) were added where indicated. P denotes probe alone. NA denotes no extract added. A radiolabelled double-stranded oligonucleotide probe corresponding to element I (A), II (B), III (C), or IV (D) was used in mobility-shift assays with 15 (A, B, and D) or 10 (C) μg of nuclear extracts prepared from fibroblasts treated with the B:B isoform of PDGF (30 ng/ml) for 1.75 h (+).

analysis using nuclear extracts from IL-1α-treated cells. As shown in Fig. 2, the IL-1α and PDGF footprint patterns are indistinguishable. An additional protected region, detected between elements III and IV in Fig. 2, did not bind any nuclear protein(s) in mobility shift assays and was not studied further (data not shown).

Synthetic oligonucleotides corresponding to elements I through IV were employed as double-stranded DNA probes in mobility shift assays. By using nuclear extracts from quiescent and PDGF-treated fibroblasts, at least one PDGF-inducible complex is noted in mobility shift assays using each individual element as the probe (Fig. 3). Consistent with the DNase I footprints, binding to elements II and IV exhibits both constitutive binding and PDGF-inducible binding components (Fig.

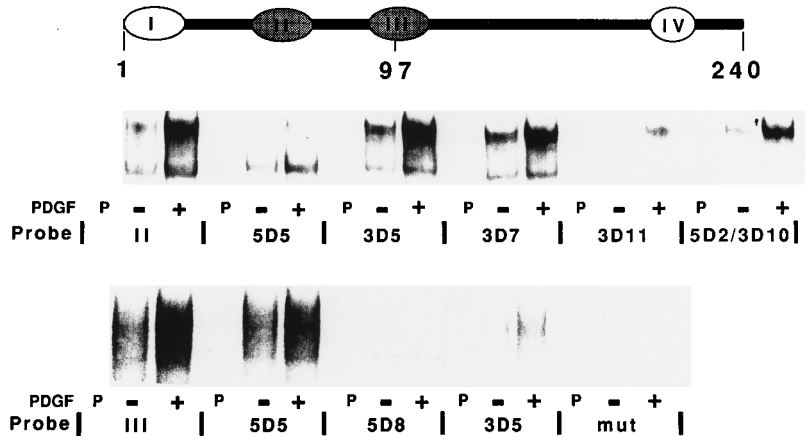

FIG. 5. PDGF inducible binding to elements II and III requires at least 15 and 18 nucleotides, respectively. (Top) Schematic diagram of 240-bp *MCP-1* enhancer fragment. Position 1 is at the 5′ end of the fragment. The relative positions of the four elements with respect to the nonoverlapping 97- and 143-bp subfragments are shown. Shaded ovals denote the probes used in these experiments. (Center) Radiolabelled double-stranded oligonucleotide probes corresponding to full-length element II and five truncated derivatives of element II were used in mobility shift assays with 15 μg of nuclear extracts prepared from quiescent fibroblasts (−) or fibroblasts treated with the B:B isoform of PDGF (30 ng/ml) for 1.75 h (+). Probe 5D5 is a truncation of element II containing a 5-nucleotide deletion at the 5′ end of element II. Probes 3D5, 3D7, and 3D11 are truncations of element II containing deletions of 5, 7, and 11 nucleotides, respectively, at the 3′ end of element II. Probe 5D2/3D10 is a truncation of element II containing a 2-nucleotide deletion at the 5′ end and a 10-nucleotide deletion at the 3′ end of element II. P denotes probe alone. (Bottom) Radiolabelled double-stranded oligonucleotide probes corresponding to full-length element III, three truncated derivatives of element III, and an 8-base mutation of element III were used in mobility shift assays with 10 μg of nuclear extracts prepared from quiescent fibroblasts (−) or fibroblasts treated with the B:B isoform of PDGF (30 ng/ml) for 1.75 h (+). Probes 5D5 and 5D8 are truncations of element III containing 5- and 8-nucleotide deletions, respectively, at the 5′ end of element III. Probe 3D5 is a truncation of element III containing a 5-nucleotide deletion at the 3′ end of element III. The mut probe contains an 8-nucleotide internal mutation of element III (GCTGCAGG changed to TAGTACTT at positions 12 to 19 of the mutant relative to the 5′ end of element III). P denotes probe alone.

3). In contrast to the footprint analysis, PDGF-inducible binding to element III is seen in mobility shift assays (compare Fig. 2, lanes 3 and 4, 6 and 7, and 9 and 10, with binding to element III in Fig. 3). One explanation for this apparent discrepancy comes from determining differences in "on" rates of binding to element III between quiescent and PDGF-treated nuclear extracts. PDGF-treated nuclear extracts have significantly greater on rates of binding to element III than nuclear extracts from quiescent fibroblasts (data not shown). For footprint analysis, larger amounts of each nuclear extract were added for longer binding incubations, thereby obscuring the differences in rates of protein binding to element III.

Elements I and IV are related to each other and bind one or more forms of the transcription factor NF-κB. In mobility shift assays, oligonucleotides corresponding to elements I and IV compete for binding to themselves and each other (Fig. 4A and D). Oligonucleotides containing two different NF-κB-binding sequences (designated NF1 and NF2 [Fig. 4]) also compete for binding to elements I and IV. Polyclonal antibodies specific for the p50 and p65 subunits of NF-κB supershift several of the complexes which bind elements I and IV (Fig. 4A and D). Specificity of antibody supershifts is demonstrated by removal of supershifts with addition of peptides used in generation of the antibodies (Fig. 4A and D, upper two arrows). Interestingly, neither element I nor NF-κB-related oligonucleotides compete for specific binding of a noninducible complex to element IV (Fig. 4D, bottom arrow).

Elements II and III are novel binding sequences and require at least 15 and 18 nucleotides, respectively, for PDGF-inducible binding to occur. Only oligonucleotides corresponding to the shift probes themselves compete for binding to elements II and III. No competition was observed with oligonucleotides (i) corresponding to element IV or (ii) containing two distinct NF-κB-binding sites (Fig. 4B and C). Oligonucleotides corresponding to element I are also unable to compete with binding to elements II and III (data not shown). No supershifts were observed with anti-p50 or anti-p65 antisera (Fig. 4B and C). Further experiments focused on elements II and III.

Steric hindrance of DNase I activity by proteins binding specifically to DNA in footprinting reactions is known to result in overestimation of the true size of protein-binding sequences. Mobility shift assays using several deletion probes of elements II and III were therefore used to more precisely delineate the sequences within elements II (which footprints as a 27-mer) and III (which footprints as a 28-mer) required for PDGF-inducible binding. Deletions of up to 7 nucleotides at the 3′ end of element II do not alter PDGF-inducible binding (Fig. 5, center). In contrast, deletion of a 5-nucleotide CCTTT sequence at the 5′ end of element II, or 11 nucleotides at the 3′ end of element II, eliminates PDGF-inducible binding (Fig. 5, center). These data suggest that PDGF-inducible binding to element II requires some portion of the 5′ CCTTT sequence. By using a probe with smaller 5′ and 3′ deletions, PDGF-inducible binding to element II is shown to require at least 15 nucleotides (Fig. 5, center; compare binding to probe 5D2/3D10, a 15-mer, with binding to unaltered element II probe).

Deletion of 8 nucleotides at the 5′ end of element III, or 5 nucleotides at the 3′ end of element III, eliminates PDGF-inducible binding to element III (Fig. 5, bottom). Deletion of 5 nucleotides at the 5′ end of element III reduces, but does not eliminate, PDGF-inducible binding to element III (Fig. 5, bottom). These data demonstrate that PDGF-inducible binding to element III is diminished or eliminated by 5-nucleotide deletions at the 5′ or 3′ ends of element III, suggesting that PDGF-inducible binding to element III requires at least 18 nucleotides. PDGF-inducible binding to element III is also eliminated by an 8-base mutation within element III (Fig. 5, bottom).

Sequence comparison revealed no known transcription factor-binding sequences closely matching the minimal sizes of elements II and III determined in Fig. 5. In particular, neither element contains *sis*-inducible factor-binding sequences (51).

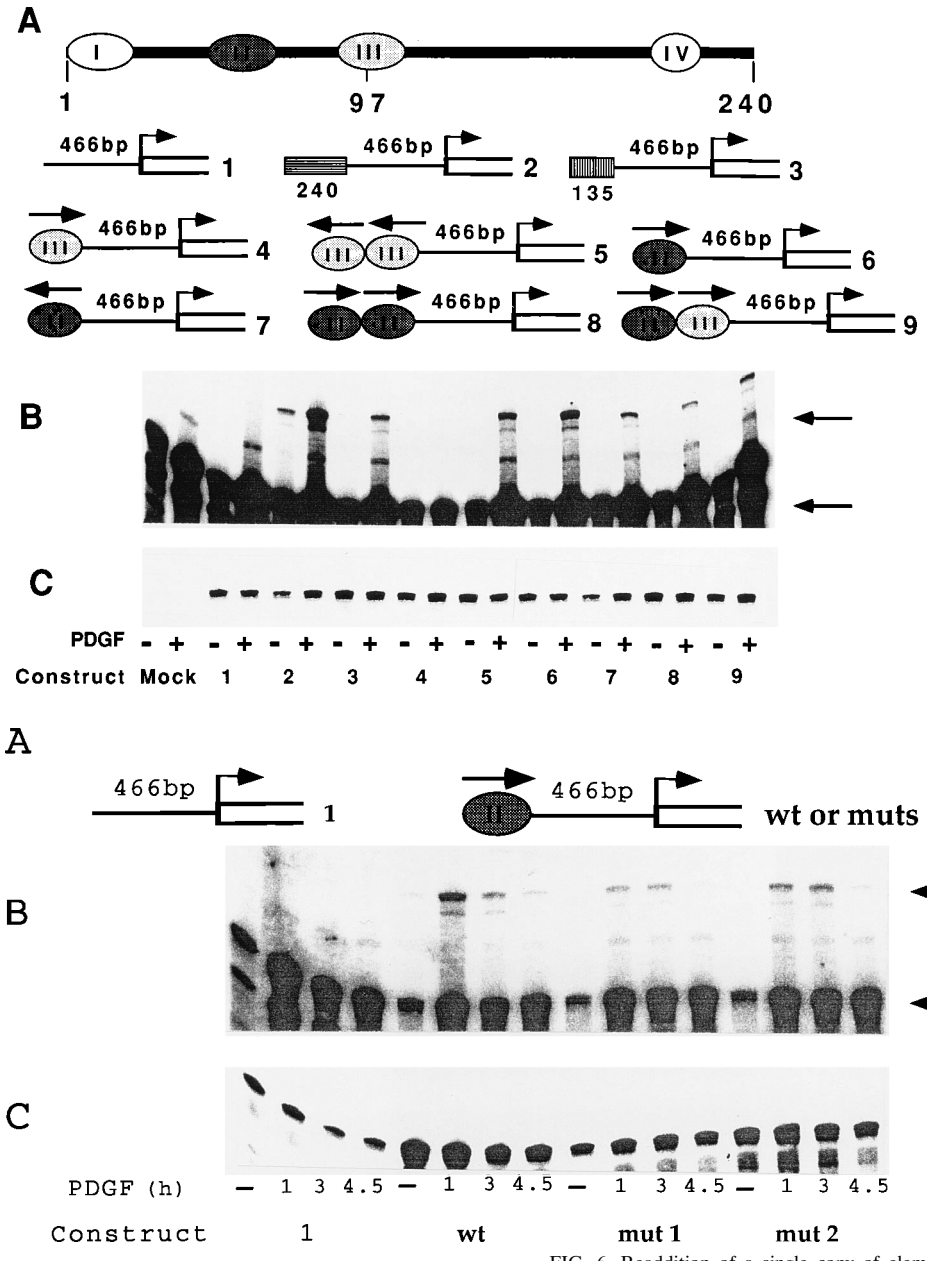

FIG. 6. Readdition of a single copy of element II is sufficient to restore PDGF inducibility to a noninducible *MCP-1* reporter gene. (Top panel) (A) Schematic diagram of 240-bp *MCP-1* enhancer fragment. Position 1 is at the 5′ end of the fragment. The relative positions of the four elements with respect to the nonoverlapping 97- and 143-bp subfragments are shown. Also shown in schematic form (construct 1) is the structure of the 5′ end of a noninducible tagged *MCP-1* reporter gene (pGMJE-1), which includes 466 bp of 5′ flanking sequences and 1.9 kb of 3′ untranslated sequences. Constructs 2 and 3 are derived from construct 1 by readdition of the shown 240- and 135-bp fragments, respectively. The 240-bp fragment is present in the distal 5′ *MCP-1* flanking sequences (with ends at −2537 and −2298 bp relative to the *MCP-1* start of transcription). The 135-bp fragment (including nucleotides 34 through 168 of the 240-bp fragment) contains both elements II and III. Both fragments are readded in the in vivo orientation. Constructs 4 through 9 are derived from construct 1 by readdition of one or two copies of element II or III as shown. A rightward-facing arrow above an element denotes readdition in the in vivo orientation. A leftward-facing arrow above an element denotes readdition in the reverse orientation. (B) RNase protection assays of 30 μg of total cellular RNA from fibroblasts trans-

A potential AP-1-binding site is present within the minimal required element II-binding sequences delineated above. Mobility shift experiments using a labelled AP-1 oligonucleotide probe, however, did not yield complexes similar to those seen with the element II probe (data not shown). Because elements II and III appear to be novel PDGF-regulated DNA-binding elements, further experiments focused on their properties.

Readdition of a single copy of element II is sufficient to restore PDGF inducibility to a noninducible *MCP-1* reporter gene. In add-back experiments, a single copy of element II, in either orientation, is sufficient to restore PDGF inducibility to a truncated, noninducible *MCP-1* gene (Fig. 6, top panel; compare the stimulated lanes of constructs 6 and 7 with construct 1). A single copy of element II functions as well as the large 135-bp subfragment (described in Fig. 1) that contains both elements II and III (Fig. 6, top panel; compare the stimulated lanes of constructs 6 and 3). With neither readdition are the resulting PDGF inductions equal to the induction obtained with the complete 240-bp enhancer fragment (Fig. 6, top panel; compare the stimulated lanes of constructs 6 and 3 with construct 2). No further increases in induction are obtained with readdition of two copies of element II or with readdition of single copies of elements II and III together (Fig. 6, top panel; compare the stimulated lanes of constructs 6, 8, and 9). Lastly, readdition of two copies of element III restores PDGF inducibility (Fig. 6, top panel, compare the stimulated lanes of constructs 5 and 1).

Readdition of a single copy of element III to the noninducible *MCP-1* reporter gene does not restore PDGF inducibility (Fig. 6, top panel; compare the stimulated lanes of constructs 4 and 1). Likewise, readdition of a single copy of element I to the same noninducible *MCP-1* reporter gene does not restore PDGF inducibility (data not shown). Taken together, these results suggest that readdition of a single copy of element II specifically restores PDGF inducibility, rather than creating a nonspecific spacer artifact.

These experiments do not address directly whether element III is necessary for a small portion of the full *MCP-1* induction observed in response to PDGF stimulation. That such a contribution by element III is minimal is strongly suggested by the result that equal PDGF inductions are obtained with constructs 6 and 3 (Fig. 6, top panel). Construct 3 contains the 135-bp subfragment (described in Figure 1), which includes elements II and III in their in vivo positions and orientations, as well as substantial amounts of flanking sequences. Were there a synergistic interaction between elements II and III, construct 3 would be expected to be inducible to a greater extent than construct 6.

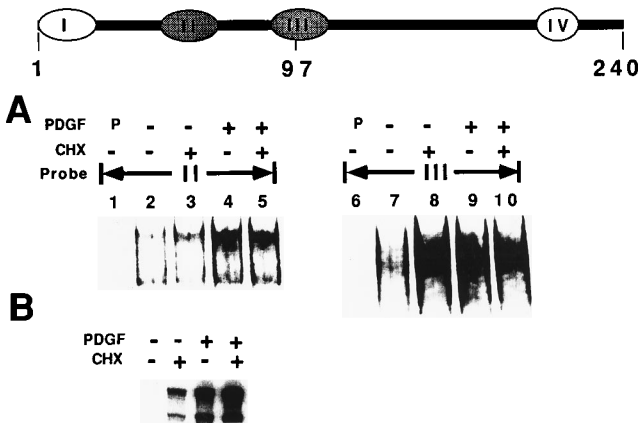

FIG. 7. PDGF-inducible binding to elements II and III occurs in the presence of cycloheximide. A schematic diagram of the 240-bp *MCP-1* enhancer fragment is shown at the top. Position 1 is at the 5′ end of the fragment. The relative positions of the four elements with respect to the nonoverlapping 97- and 143-bp subfragments are shown. Shaded ovals denote the probes used in these experiments. (A) Radiolabelled double-stranded oligonucleotide probes corresponding to elements II and III were used in mobility shift assays with 15 μg (element II) or 10 μg (element III) of nuclear extracts prepared from quiescent fibroblasts (−) or fibroblasts treated with the B:B isoform of PDGF (30 ng/ml) for 1.75 h (+), in the presence or absence of CHX (added at 10 μg/ml). CHX was added 30 min prior to the addition of PDGF. P denotes probe alone. Increases in upper complex binding to element II of 1.6-, 3.8-, and 3.6-fold were observed in the CHX-, PDGF-, and PDGF-CHX-treated groups, respectively. Increases in binding to element III of 6.5-, 5.4-, and 4.6-fold were observed in the CHX-, PDGF-, and PDGF-CHX-treated groups, respectively. (B) RNase protection assays of 10 μg of total cellular RNA prepared from the four groups of fibroblasts described for panel A, using a murine MCP-1 riboprobe. Increases in *MCP-1* RNA of 38-, 190-, and 380-fold were observed in the CHX-, PDGF-, and PDGF-CHX-treated groups, respectively.

Mutational analysis of element II. Two site-directed mutants of element II were generated. In one mutant (mut1) the extreme 5′ end of element II is altered. The 5′ end of element II is shown in Fig. 2 to be part of a PDGF-inducible footprint delineating element II. In the second mutant, bases 13 to 20 of element II (mut2) are altered. Wild-type sequences altered in both mutants are required for PDGF-inducible binding to element II (Fig. 5). Using either element II mutant as a competitor in mobility shift assays (at a 100-fold excess) resulted in no significant decreases in PDGF-inducible binding to element II (data not shown). The sequences of both mutations are given in Materials and Methods.

Time courses of PDGF stimulation, using add-back constructs containing wild-type element II or the two site-directed mutants in transient transfections, were determined (Fig. 6, middle and bottom panels). PDGF stimulation of an *MCP-1* add-back construct containing a single copy of wild-type element II parallels the initial kinetics of endogenous *MCP-1* induction with maximal induction at 1 h of PDGF addition but exhibits greater decreases in *MCP-1* RNA levels at 3 and 4.5 h of stimulation (Fig. 6, middle and bottom panels). In contrast, mutants 1 and 2 exhibit considerably decreased PDGF inductions at 1 h of stimulation (91 and 79% decreases, respectively,

fected with 50 μg of the shown constructs or mock transfected, allowed to become quiescent, and then either not exposed (−) or exposed (+) to the B:B isoform of PDGF (30 ng/ml) for 2 h. The arrows indicate the 305- and 241-nucleotide protected fragments corresponding to expression of transfected *MCP-1* constructs and endogenous *MCP-1*, respectively. PhosphorImager images were designed to optimally demonstrate expression of the transfected constructs. Equal inductions of construct 2 and endogenous *MCP-1* were observed in all experiments. (C) RNase protection assays of 10 μg of total cellular RNA from the transfections shown in panel B with an alpha-globin riboprobe. (Middle panel) (A) Construct 1 is as described for the top panel of this figure. Wild-type (wt) or mutant (mut1 or mut 2) element II constructs are derived from construct 1 by the addition of the relevant oligonucleotides. A rightward-facing arrow above an element denotes readdition in the in vivo orientation. Sequences for each mutant are given in Materials and Methods. (B) RNase protection assays of 30 μg of total cellular RNA from fibroblasts transfected with 50 μg of the shown constructs, allowed to become quiescent, and then either not exposed (−) or exposed to the B:B isoform of PDGF (30 ng/ml) for the indicated times (in hours). The arrows indicate the 305-nucleotide (top arrow) and 241-nucleotide (bottom arrow) protected fragments corresponding to expression of transfected *MCP-1* constructs and endogenous *MCP-1*, respectively. PhosphorImager images were designed to optimally demonstrate expression of the transfected constructs. (C) RNase protection assays of 10 μg of total cellular RNA from the transfections shown in panel B with an alpha-globin riboprobe. (Bottom panel) Graphical representation of the data presented in the middle panel of this figure. wt (■), mut 1 (◆), and mut 2 (●) are the element II add-back constructs described in part A of the middle panel of this figure. Quantitation was performed on a PhosphorImager after a 5-day exposure of the gel. Counts for the endogenous *MCP-1* gene (endog MCP-1 [▲]) are reduced by a factor of 10^{-6}. All other counts are reduced by a factor of 10^{-5}.

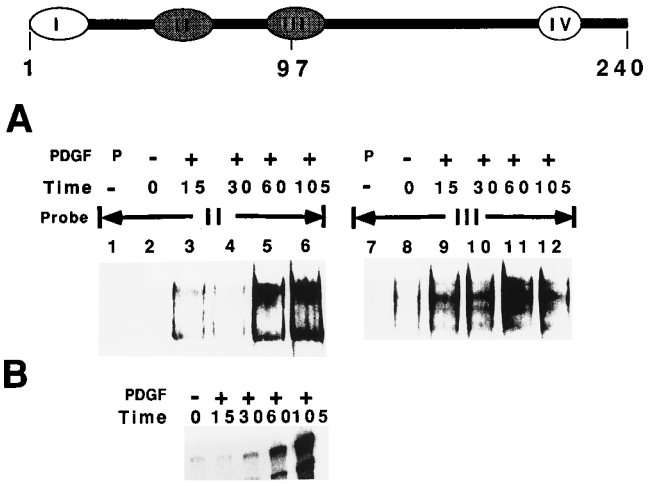

FIG. 8. Time course of PDGF-inducible binding to elements II and III. A schematic diagram of the 240-bp MCP-1 enhancer fragment is shown at the top. Position 1 is at the 5′ end of the fragment. The relative positions of the four elements with respect to the nonoverlapping 97- and 143-bp subfragments are shown. Shaded ovals denote the probes used in these experiments. (A) Radiolabelled double-stranded oligonucleotide probes corresponding to elements II and III were used in mobility shift assays with 15 μg (element II) or 10 μg (element III) of nuclear extracts prepared from quiescent fibroblasts (−) or fibroblasts treated with the B:B isoform of PDGF (30 ng/ml) for the indicated times (in minutes). P denotes probe alone. Increases in upper complex binding to element II of 1.6-, 1.8-, 5.0-, and 8.4-fold were observed for the 15-, 30-, 60-, and 105-min groups, respectively. Increases in binding to element III of 4.0-, 4.5-, 8.7-, and 4.9-fold were observed for the 15-, 30-, 60-, and 105-min groups, respectively. (B) RNase protection assays of 10 μg of total cellular RNA prepared from the same groups of fibroblasts described for panel A, using a murine *MCP-1* riboprobe. Increases in *MCP-1* RNA of 0-, 2.5-, 20-, and 110-fold were observed for the 15-, 30-, 60-, and 105-min groups, respectively.

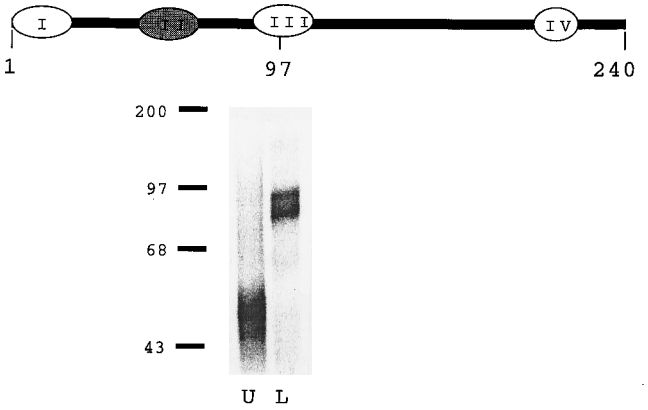

FIG. 9. UV cross-linking of proteins binding to element II. A schematic diagram of the 240-bp *MCP-1* enhancer fragment is shown at the top. Position 1 is at the 5′ end of the fragment. The relative positions of the four elements with respect to the nonoverlapping 97- and 143-bp subfragments are shown. The shaded oval denotes the element used in the cross-linking experiments. A radiolabelled 5-bromodeoxyuridine-substituted double-stranded oligonucleotide probe corresponding to element II (top strand substituted) was used in mobility shift assays with nuclear extracts prepared from fibroblasts treated with the B:B isoform of PDGF (30 ng/ml) for 1.75 h. Complexes were electrophoresed on 4% nondenaturing polyacrylamide gels followed by UV cross-linking (1,000 mJ). PDGF-inducible upper (U) and noninducible lower (L) DNA-protein complexes binding element II were excised from the nondenaturing gel and resolved by electrophoresis in a sodium dodecyl sulfate–8% polyacrylamide protein gel. Molecular mass standards (in kilodaltons) are shown on the left. Similar results were observed with 500-mJ UV irradiation (data not shown). Similar but weaker cross-linking was observed with a bottom-strand, 5-bromodeoxyuridine-substituted element II probe (data not shown).

compared with that of the wild-type element II construct [Fig. 6, middle and bottom panels]). With both mutants, *MCP-1* RNA levels are maximally elevated at 1 h but remain at these levels through at least 3 h of PDGF stimulation (Fig. 6, middle and bottom panels). This is in contrast to the wild-type element II-containing construct, which exhibits a marked decrease in *MCP-1* RNA levels by 3 h of PDGF stimulation. These differences could reflect a small degree of similar PDGF-inducible proteins binding in vivo to both mutants and wild-type element II. Alternatively, PDGF induction of each mutant-containing construct could reflect activation of transcription through a different enhancer present in the mutants (such as the minimally altered AP-1 site present in each mutant). It should be noted that endogenous *MCP-1* RNA levels remained elevated for at least 4.5 h of PDGF stimulation, whereas *MCP-1* levels from the transfected wild-type element II-containing construct returned to near baseline levels by 4.5 h of stimulation (Fig. 6, middle and bottom panels). Hence, a single copy of element II alone is capable of restoring the initial high degree of *MCP-1* induction in response to PDGF but is not responsible for the sustained component of *MCP-1* induction after PDGF stimulation.

In summary, two element II mutants which do not inhibit PDGF-inducible binding to element II confer significantly decreased PDGF inducibility to a truncated noninducible *MCP-1* construct (Fig. 6, middle and bottom panels). These data establish a strong association between PDGF-inducible protein(s) binding to element II and PDGF-mediated induction of *MCP-1* RNA. Because of the central role element II appears to play in PDGF induction of *MCP-1*, the following sections focus on the binding of the PDGF-inducible protein(s) to element II. Parallel experiments involving PDGF-inducible binding to element III are reported as well.

PDGF-inducible protein binding to element II occurs in the presence of cycloheximide and with kinetics similar to those of PDGF induction of *MCP-1* RNA. PDGF-inducible binding to element II in mobility shift assays is equally pronounced in the absence and presence of cycloheximide (CHX) (Fig. 7A). A small increase in binding to element II is also observed in nuclear extracts from CHX-treated fibroblasts (Fig. 7A). Changes in binding to element II in mobility shift assays closely parallel changes in *MCP-1* RNA levels from fibroblasts treated with CHX, PDGF, or both (compare binding in Fig. 7A, left panel, with that in Fig. 7B). In contrast, binding to element III in mobility shift assays is equal in nuclear extracts prepared from fibroblasts treated with CHX, PDGF, or both, a result that correlates poorly with the differences in *MCP-1* RNA levels shown in Fig. 7B.

PDGF-inducible binding to element II in mobility shift assays occurs with delayed kinetics. Significant increases in binding to element II are seen with nuclear extracts from fibroblasts treated with PDGF for at least 60 min (Fig. 8A, left panel). *MCP-1* RNA induction after PDGF treatment occurs with similarly delayed kinetics (compare binding changes in Fig. 8A, left panel, with changes in *MCP-1* RNA levels in Fig. 8B). In contrast, PDGF-stimulated binding to element III in mobility shift assays is nearly maximal after a 15-min treatment of fibroblasts with PDGF (Fig. 8A, right panel). It should be noted that the kinetics of *MCP-1* induction in BALB/c-3T3 cells upon PDGF stimulation are more delayed than in NIH 3T3 cells (Fig. 6, middle and bottom panels, and 8B). The reason(s) for these slight differences is unknown.

PDGF-inducible binding to element II involves a 30-kDa protein. Protein complexes binding to element II in mobility shift assays consist of two components, (i) a faster migrating

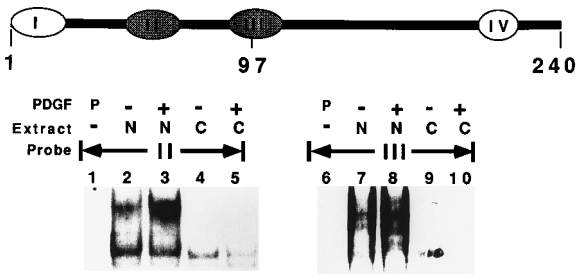

FIG. 10. PDGF-inducible binding to elements II and III is detected in nuclear extracts only. (Top) Schematic diagram of 240-bp *MCP-1* enhancer fragment. Position 1 is at the 5′ end of the fragment. The relative positions of the four elements with respect to the nonoverlapping 97- and 143-bp subfragments are shown. Shaded ovals denote the probes used in these experiments. (Bottom) A radiolabelled double-stranded oligonucleotide probe corresponding to element II (left panel) or III (right panel) was used in mobility shift assays with 15 (element II) or 10 (element III) μg of nuclear (N) or cytoplasmic (C) extracts prepared from quiescent fibroblasts (−) or fibroblasts treated with the B:B isoform of PDGF (30 ng/ml) for 1.75 h (+). P denotes probe alone. A 3.9- or 2.1-fold increase in upper complex binding to element II or III, respectively, after PDGF stimulation was observed in the nuclear extract group.

minimally PDGF-inducible (lower) complex and (ii) a more slowly migrating strongly PDGF-inducible (upper) complex (Fig. 3 and 5). UV-mediated DNA-protein cross-linking was performed on both complexes. The strongly PDGF-inducible upper complex contains a single 48-kDa cross-linked species (Fig. 9). Correcting for the molecular mass of the probe (18 kDa), the upper element II-binding complex contains a 30-kDa protein. The lower element II-binding complex contains proteins with approximate molecular masses of 62 and 68 kDa after correcting for the molecular mass of the probe (Fig. 9). Whether the 62- and 68-kDa proteins are related to each other structurally is unknown at this time. No cross-linking is observed in the absence of UV irradiation of the gel (data not shown).

PDGF-inducible binding to element II is present in nuclear extracts only. Nuclear and cytoplasmic extracts from either quiescent or PDGF-treated fibroblasts were used in mobility shift assays. PDGF-inducible (upper complex) binding to element II in mobility shift assays is detected in nuclear extracts only (Fig. 10, left panel). In contrast, noninducible (lower complex) binding to element II is present in both nuclear and cytoplasmic extracts (Fig. 10, left panel).

PDGF-inducible binding to element III in mobility shift assays is also present in nuclear extracts only (Fig. 10, right panel). As a control for integrity of the cytoplasmic extracts used in these experiments, we assayed for binding of NF-κB, a transcription factor known to be activated in the cytoplasm after a stimulus with subsequent translocation to the nucleus (3, 29). PDGF-inducible binding of NF-κB to elements I and IV in mobility shift assays is seen with all cytoplasmic extracts used in these experiments (data not shown).

PDGF-inducible binding to element II involves a serine/threonine phosphoprotein. Nuclear extracts from PDGF-treated fibroblasts were used in mobility supershift assays in conjunction with three monoclonal antisera specific for the phosphorylated forms of serine, threonine, and tyrosine. PDGF-inducible (upper complex) binding to element II is supershifted, in a dose-dependent manner, in the presence of monoclonal anti-phosphoserine or anti-phosphothreonine antibodies (Fig. 11A). PDGF-inducible binding to element II is

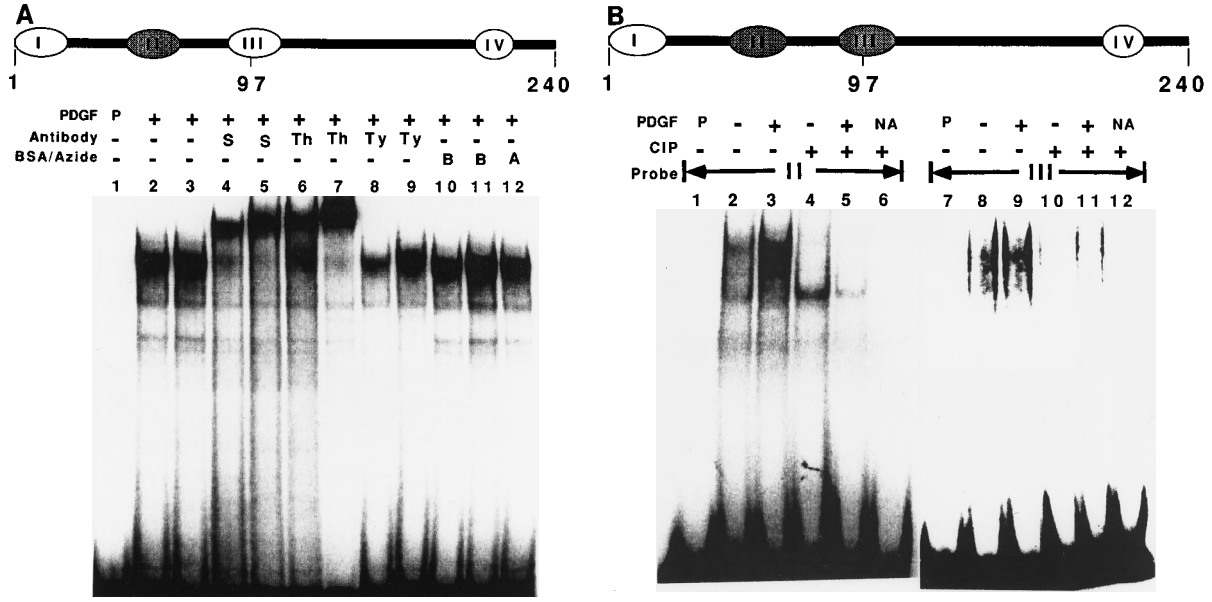

FIG. 11. PDGF-inducible binding to element II involves a serine/threonine phosphoprotein. A schematic form of the 240-bp MCP-1 enhancer fragment is shown at the top of both panels. Position 1 is at the 5′ end of the fragment. The relative positions of the four elements with respect to the nonoverlapping 97- and 143-bp subfragments are shown. Shaded ovals denote the probes used in these experiments. (A) A radiolabelled double-stranded oligonucleotide probe corresponding to element II was used in mobility-shift assays with 15 μg of nuclear extracts prepared from fibroblasts treated with the B:B isoform of PDGF (30 ng/ml) for 1.75 h (+). S, monoclonal antiphosphoserine antibodies added to supershifts (11 and 22 μg in lanes 4 and 5, respectively); Th, monoclonal antiphosphothreonine antibodies added to supershifts (9 and 18 μg in lanes 6 and 7, respectively); Ty, monoclonal antiphosphotyrosine antibodies added to supershifts (10 and 23 μg in lanes 8 and 9, respectively); BSA, bovine serum albumin added (25 and 100 μg in lanes 10 and 11, respectively); Azide, sodium azide added to a final concentration of 0.05%; P, probe alone. (B) Radiolabelled double-stranded oligonucleotide probes corresponding to elements II and III were used in mobility-shift assays with 15 μg (element II) or 10 μg (element III) of nuclear extracts prepared from quiescent fibroblasts (−) or fibroblasts treated with the B:B isoform of PDGF (30 ng/ml) for 1.75 h (+). CIP pretreatment (1 U per μl) was done for 30 min at 30°C. P, probe alone; NA, no extract added. An 8.7- or 2.9-fold increase in upper complex binding to element II or III, respectively, after PDGF-stimulation was observed in the absence of CIP pretreatment.

not affected by the addition of monoclonal anti-phosphotyrosine antisera (Fig. 11A). As each of the monoclonal antisera is provided as ascites fluid, the latter results with monoclonal anti-phosphotyrosine antisera constitute a control for the specificity of the supershifts noted with the monoclonal anti-phosphoserine and anti-phosphothreonine antibodies. In contrast, lower complex (noninducible) binding to element II is not supershifted with any of the antisera (Fig. 11A).

Additional experiments addressed whether phosphorylation is necessary for binding to element II. Pretreatment of nuclear extracts from quiescent or PDGF-treated fibroblasts with CIP completely removed PDGF-inducible (upper complex) binding to element II (Fig. 11B). In contrast, noninducible (lower complex) binding to element II is not removed by CIP treatment (Fig. 11B). Similar results are seen with CIP treatment of PDGF-inducible proteins binding to element III (Fig. 11B). As a control for possible nonspecific proteolysis resulting from CIP treatment, binding of NF-κB in mobility shift assays was examined. No significant decreases in PDGF-inducible NF-κB binding in mobility shift assays are seen after treatment with CIP (data not shown). Finally, pretreatment of nuclear extracts from PDGF-treated fibroblasts with a tyrosine phosphatase derived from *Y. enterocolitica* did not remove PDGF-inducible binding to element II (data not shown).

DISCUSSION

A new PDGF-regulated genomic element mediates induction of the *MCP-1* gene. *cis*- and *trans*-acting regulatory elements for c-*fos* and other fast immediate-early genes have been well characterized (22, 42, 46, 51). The mechanism(s) underlying PDGF-mediated induction of a large second class of immediate-early genes, induced with slower kinetics than the c-*fos* gene and including the c-*myc* and *MCP-1* genes, is less well resolved. Herein we describe a pair of novel PDGF-regulated *cis*-acting elements (elements II and III) that mediate *MCP-1* induction. Readdition of a single copy of element II restores PDGF inducibility to an otherwise noninducible *MCP-1* reporter construct (Fig. 6). Element III restores PDGF inducibility only when added back in two copies. Although element III is therefore likely to be silent in PDGF-mediated induction of *MCP-1* (which contains only one copy of element III), other genes containing two copies of this element could be PDGF inducible. Both elements are contained within a 240-bp enhancer fragment found 2.3 kb upstream of the *MCP-1* start of transcription.

Two additional PDGF-responsive *cis*-acting elements are also present within the 240-bp *MCP-1* enhancer. Both elements (I and IV) contain homologous sequences and bind several forms of the transcription factor NF-κB. In addition, element IV also binds a noninducible protein complex which does not bind to element I (Fig. 4). Readdition of a single copy of element IV or two copies of element I is sufficient to restore PDGF inducibility to a noninducible *MCP-1* reporter construct (data not shown). Readdition of single copies of element II or IV to a noninducible *MCP-1* reporter gene restores in each case approximately 50% of the full level of PDGF induction obtained with readdition of the complete 240-bp enhancer (Fig. 6, top panel, and data not shown). Taken together, these data suggest that PDGF induction of *MCP-1* proceeds through two independent pathways in fibroblasts. One pathway involves activation of the widely present transcription factor NF-κB. A second pathway involves activation through a novel genomic element (element II). NF-κB has also been suggested recently to be involved in IL-1α- and tumor necrosis factor alpha-mediated induction of the *MGSA/gro* (or *KC*) gene (45).

PDGF-inducible binding to element II includes a 30-kDa protein and a serine/threonine phosphoprotein. UV cross-linking experiments detect a single 30-kDa protein in the PDGF-inducible (upper) element II binding complex (Fig. 9). PDGF-inducible binding to element II is detected only in nuclear extracts (Fig. 10) and is specifically supershifted with monoclonal antibodies to phosphoserine and phosphothreonine (Fig. 11). Additionally, CIP pretreatment selectively removes the PDGF-inducible upper element II-binding complex (Fig. 11). Taken together, these data suggest that the PDGF-activated binding to element II includes one or more nuclear-restricted serine/threonine phosphoproteins and that a phosphate group(s) is required for PDGF-activated binding to element II. Whether the 30-kDa protein (p30) detected by UV cross-linking is identical to the serine/threonine phosphoprotein detected in the antibody supershift experiments is unknown at this time. Significantly, after treatment with PDGF, (i) stimulation of binding to element II in nuclear extracts and (ii) induction of *MCP-1* gene expression occur with similar delayed time courses (Fig. 8).

Two mutants of element II which confer decreased PDGF inducibility, as well as significantly different kinetics of induction, to a truncated noninducible *MCP-1* construct in transient transfections were generated (Fig. 6, middle and bottom). The element II mutants neither compete with PDGF-inducible (p30) binding to element II in mobility shift assays nor bind complexes comigrating with the PDGF-inducible p30-containing complex when used as the probe in mobility shift assays (data not shown). Taken together, these data are strongly consistent with a causal relationship between PDGF-inducible protein(s) binding to element II and PDGF-mediated induction of *MCP-1* RNA.

We propose the following model for PDGF induction of *MCP-1* in BALB/c-3T3 fibroblasts. Binding of PDGF to its membrane receptor initiates a signal culminating in phosphorylation of an intranuclear 30-kDa protein (p30) on serine and threonine. Time course studies (Fig. 8) suggest a 1-h delay in phosphorylation of p30, possibly due to delayed initiation of second messenger generation at the receptor level or to a complex intracytoplasmic sequence of reactions preceding phosphorylation of p30. Active phosphorylated p30 binds to element II and can then cooperate with proximal transcription machinery to initiate transcription of *MCP-1*. Whether p30 binds element II as a single molecule or as a dimer is unknown at present. Additional 62- and 68-kDa element II-binding proteins are present in both nuclear and cytoplasmic compartments but do not appear to be a part of the PDGF-inducible complex binding element II and are therefore not likely to play a role in PDGF induction of *MCP-1* (Fig. 9). At present we cannot exclude the possibility that more than one phosphoprotein is involved in PDGF-inducible binding to element II. While this model is not the only one consistent with the results presented herein, it is the simplest.

Given the marked differences in kinetics of PDGF induction between c-*fos* and *MCP-1*, it is not surprising that the mechanisms of PDGF induction for the two immediate-early genes appear to share few details in common. Lastly, given the general role that the serum response element and sis-inducible element sequences appear to play in serum and PDGF induction of many fast immediate-early genes, it is tempting to speculate that element II may play a similar general role for multiple members of the slow-kinetics subset of immediate-early genes in addition to *MCP-1*.

ACKNOWLEDGMENTS

We thank Yuan-di Halvorsen for helpful discussions and Alan D'Andrea, Rolf G. Freter, Barrett Rollins, Kerry Reinertsen, and Thomas Roberts for critical reading of the manuscript.

R.R.F. is a recipient of a fellowship from the National Institutes of Health (5 F32 GM14091). This research was supported by grant CA22042 from the National Institutes of Health to C.D.S.

REFERENCES

1. **Almendral, J. M., D. Sommer, H. Macdonald-Bravo, J. Burckhardt, J. Perera, and R. Bravo.** 1988. Complexity of the early genetic response to growth factors in mouse fibroblasts. Mol. Cell. Biol. **8:**2140–2148.
2. **Ausubel, F. M., R. Brent, R. E. Kingston, D. D. Moore, J. G. Seidman, and J. A. Smith (ed.).** 1990. Current protocols in molecular biology. Greene Publishing Associates and Wiley-Interscience, New York.
3. **Baeuerle, P. A.** 1991. The inducible transcription activator NF-κB: regulation by distinct protein subunits. Biochim. Biophys. Acta **1072:**63–80.
4. **Berkowitz, L. A., K. T. Riabowol, and M. Z. Gilman.** 1989. Multiple sequence elements of a single functional class are required for cyclic AMP responsiveness of the mouse c-*fos* promoter. Mol. Cell. Biol. **9:**4272–4281.
5. **Chirgwin, J. M., A. E. Przybyla, R. J. Macdonald, and W. J. Rutter.** 1979. Isolation of biologically active ribonucleic acid from sources enriched in ribonuclease. Biochemistry **18:**5294–5299.
6. **Chittenden, T., D. M. Livingston, and J. A. DeCaprio.** 1993. Cell cycle analysis of E2F in primary human T cells reveals novel E2F complexes and biochemically distinct forms of free E2F. Mol. Cell. Biol. **13:**3975–3983.
7. **Christy, B., and D. Nathans.** 1989. Functional serum response elements upstream of the growth factor-inducible gene *zif268*. Mol. Cell. Biol. **9:**4889–4895.
8. **Cochran, B. H., A. C. Reffel, and C. D. Stiles.** 1983. Molecular cloning of gene sequences regulated by platelet-derived growth factor. Cell **33:**939–947.
9. **Dean, M., R. A. Levine, W. Ran, M. S. Kindy, G. E. Sonenshein, and J. Campisi.** 1986. Regulation of c-myc transcription and mRNA abundance by serum growth factors and cell contact. J. Biol. Chem. **261:**9161–9166.
10. **DeBelle, I., P. R. Walker, I. C. P. Smith, and M. Sikorska.** 1991. Identification of a multiprotein complex interacting with the c-*fos* serum response element. Mol. Cell. Biol. **11:**2752–2759.
11. **Dignam, J. D., R. M. Lebovitz, and R. G. Roeder.** 1983. Accurate transcription initiation by RNA polymerase II in a soluble extract from isolated mammalian nuclei. Nucleic Acids Res. **11:**1475–1489.
12. **Fisch, T. M., R. Prywes, M. C. Simon, and R. G. Roeder.** 1989. Multiple sequence elements in the c-fos promoter mediate induction by cAMP. Genes Dev. **3:**198–211.
13. **Freter, R. R., J.-C. Irminger, J. A. Porter, S. D. Jones, and C. D. Stiles.** 1992. A novel 7-nucleotide motif located in 3′ untranslated sequences of the immediate-early gene set mediates platelet-derived growth factor induction of the JE gene. Mol. Cell. Biol. **12:**5288–5300.
14. **Gilman, M. Z.** 1988. The c-fos serum response element responds to protein kinase C-dependent and -independent signals but not to cyclic AMP. Genes Dev. **2:**394–402.
15. **Graham, R., and M. Gilman.** 1991. Distinct protein targets for signals acting at the c-fos serum response element. Science **251:**189–192.
16. **Greenberg, M. E., Z. Siegfried, and E. B. Ziff.** 1987. Mutation of the c-*fos* gene dyad symmetry element inhibits serum inducibility of transcription in vivo and the nuclear regulatory factor binding in vitro. Mol. Cell. Biol. **7:**1217–1225.
17. **Greenberg, M. E., and E. B. Ziff.** 1984. Stimulation of 3T3 cells induces transcription of the c-fos proto-oncogene. Nature (London) **311:**433–437.
18. **Hall, D. J., J. A. Alberta, and C. D. Stiles.** 1989. Labile repressors are involved in the transcriptional control of PDGF-responsive genes. Oncol. Res. **1:**177–184.
19. **Hall, D. J., C. Brownlee, and C. D. Stiles.** 1989. Interleukin-1 is a potent regulator of JE and KC gene expression in quiescent BALB-c fibroblasts. J. Cell. Physiol. **141:**154–159.
20. **Hall, D. J., S. D. Jones, D. R. Kaplan, M. Whitman, B. J. Rollins, and C. D. Stiles.** 1989. Evidence for a novel signal transduction pathway activated by platelet-derived growth factor and by double-stranded RNA. Mol. Cell. Biol. **9:**1705–1713.
21. **Hall, D. J., and C. D. Stiles.** 1987. Platelet-derived growth factor-inducible genes respond differentially to at least two distinct intracellular second messengers. J. Biol. Chem. **262:**15302–15308.
22. **Hayes, T. E., A. M. Kitchen, and B. H. Cochran.** 1987. Inducible binding of a factor to the c-fos regulatory region. Proc. Natl. Acad. Sci. USA **84:**1272–1276.
23. **Herschman, H. R.** 1991. Primary response genes induced by growth factors and tumor promoters. Annu. Rev. Biochem. **60:**281–319.
24. **Kawahara, R. S., Z.-W. Deng, and T. F. Deuel.** 1991. Glucocorticoids inhibit the transcriptional induction of JE, a platelet-derived growth factor-inducible gene. J. Biol. Chem. **266:**13261–13266.
25. **Kelly, K., B. H. Cochran, C. D. Stiles, and P. Leder.** 1983. Cell-specific regulation of the c-myc gene by lymphocyte mitogens and platelet-derived growth factor. Cell **35:**603–610.
26. **Kelly, K., and U. Siebenliest.** 1988. Mitogenic activation of normal T cells leads to increased initiation of transcription in the c-myc locus. J. Biol. Chem. **263:**4828–4831.
27. **Lau, L. F., and D. Nathans.** 1985. Identification of a set of genes expressed during the G0/G1 transition of cultured mouse cells. EMBO J. **4:**3145–3151.
28. **Lau, L. F., and D. Nathans.** 1987. Expression of a set of growth-related immediate early genes in BALB/c 3T3 cells: coordinate regulation with c-fos and c-myc. Proc. Natl. Acad. Sci. USA **84:**1182–1186.
29. **Lenardo, M. J., and D. Baltimore.** 1989. NF-κB: a pleiotropic mediator of inducible and tissue-specific gene control. Cell **58:**227–229.
30. **Melton, D. A., P. A. Krieg, M. R. Rebagliati, T. Maniatis, K. Zinn, and M. R. Green.** 1984. Efficient *in vitro* synthesis of biologically active RNA and RNA hybridization probes from plasmids containing a bacteriophage Sp6 promoter. Nucleic Acids Res. **12:**7035–7056.
31. **Misra, R. P., V. M. Rivera, J. M. Wang, P. Fan, and M. E. Greenberg.** 1991. The serum response factor is extensively modified by phosphorylation following its synthesis in serum-stimulated fibroblasts. Mol. Cell. Biol. **11:**4545–4554.
32. **Norman, C., M. Runswick, R. Pollock, and R. Treisman.** 1988. Isolation and properties of cDNA clones encoding SRF, a transcription factor that binds to the c-fos serum response element. Cell **55:**989–1003.
33. **Perez-Albuerne, E. D., G. Schatteman, L. K. Sanders, and D. Nathans.** 1993. Transcriptional regulatory elements downstream of the JunB gene. Proc. Natl. Acad. Sci. USA **90:**11960–11964.
34. **Pledger, W. J., C. D. Stiles, H. N. Antoniades, and C. D. Scher.** 1977. Induction of DNA synthesis in BALB/c-3T3 cells by serum components: reevaluation of the commitment process. Proc. Natl. Acad. Sci. USA **74:**4481–4485.
35. **Prywes, R., and R. G. Roeder.** 1986. Inducible binding of a factor to the c-fos enhancer. Cell **47:**777–784.
36. **Prywes, R., and R. G. Roeder.** 1987. Purification of the c-*fos* enhancer-binding protein. Mol. Cell. Biol. **7:**3482–3489.
37. **Qureshi, S. A., X. Cao, V. P. Sukatme, and D. A. Foster.** 1991. v-src activates mitogen-responsive transcription factor egr-1 via serum response elements. J. Biol. Chem. **266:**10802–10806.
38. **Rameh, L. E., and M. C. S. Armelin.** 1992. Downregulation of JE and KC genes by glucocorticoids does not prevent the $G_0 \rightarrow G_1$ transition in BALB/3T3 cells. Mol. Cell. Biol. **12:**4612–4621.
39. **Rollins, B. J., E. D. Morrison, and C. D. Stiles.** 1988. Cloning and expression of JE, a gene inducible by platelet-derived growth factor and whose product has cytokine-like properties. Proc. Natl. Acad. Sci. USA **85:**3738–3742.
40. **Rollins, B. J., P. Stier, T. Ernst, and G. G. Wong.** 1989. The human homolog of the JE gene encodes a monocyte secretory protein. Mol. Cell. Biol. **9:**4697–4695.
41. **Rollins, B. J., and C. D. Stiles.** 1989. Serum-inducible genes. Adv. Cancer Res. **53:**1–31.
42. **Rupprecht, H. D., V. P. Sukhatme, J. Lacy, R. B. Sterzel, and D. L. Coleman.** 1993. PDGF-induced egr-1 expression in rat mesangial cells is mediated through upstream serum response elements. Am. J. Physiol. **265:**351–360.
43. **Sanger, F., S. Nicklen, and A. R. Coulson.** 1977. DNA sequencing with chain-terminating inhibitors. Proc. Natl. Acad. Sci. USA **74:**5463–5467.
44. **Sassone-Corsi, P., J. Visvader, L. Ferland, P. L. Mellon, and I. M. Verma.** 1988. Induction of proto-oncogene fos transcription through the adenylate cyclase pathway: characterization of a cAMP-responsive element. Genes Dev. **2:**1529–1538.
45. **Shattuck, R. L., L. D. Wood, G. J. Jaffe, and A. Richmond.** 1994. MGSA/GRO transcription is differentially regulated in normal retinal pigment epithelial and melanoma cells. Mol. Cell. Biol. **14:**791–802.
46. **Silvennoinen, O., C. Schindler, J. Schlessinger, and D. E. Levy.** 1993. Ras-independent growth factor signaling by transcription factor tyrosine phosphorylation. Science **261:**1736–1739.
47. **Treisman, R.** 1985. Transient accumulation of c-fos RNA following serum stimulation requires a conserved 5′ element and c-fos 3′ sequences. Cell **42:**889–902.
48. **Treisman, R.** 1986. Identification of a protein-binding site that mediates transcriptional response of the c-fos gene to serum factors. Cell **46:**567–574.
49. **Treisman, R.** 1987. Identification and purification of a polypeptide that binds to the c-fos serum response element. EMBO J. **6:**2711–2717.
50. **Treisman, R.** 1990. The SRE: a growth factor responsive transcriptional regulator. Semin. Cancer Biol. **1:**47–58.
51. **Wagner, B. J., T. E. Hayes, C. J. Hoban, and B. H. Cochran.** 1990. The SIF binding element confers sis/PFGF inducibility onto the c-fos promoter. EMBO J. **9:**4477–4484.
52. **Zinn, K., D. DiMaio, and T. Maniatis.** 1983. Identification of two distinct regulatory regions adjacent to the human β-interferon gene. Cell **34:**865–879.